WATER RESOURCES RESEARCH, VOL. 49, 7350–7365, doi:10.1002/2012WR012853, 2013

A partitioned update scheme for state-parameter estimation of distributed hydrologic models based on the ensemble Kalman filter

Xianhong Xie[1,2] and Dongxiao Zhang[2]

Received 24 August 2012; revised 17 October 2013; accepted 19 October 2013; published 14 November 2013.

[1] Sequential data assimilation methods, such as the ensemble Kalman filter (EnKF), provide a general framework to account for various uncertainties in hydrologic modeling, simultaneously estimating dynamic states and model parameters with a state augmentation technique. But this technique suffers from spurious correlation for impulse responses, such as the rainfall-runoff process, especially in the case of high-dimensional state spaces containing various parameters. This paper presents a partitioned forecast-update scheme based on the EnKF to reduce the degree of freedom of the high-dimensional state space and to correctly capture covariances between states and parameters. In this update scheme, the parameter set is partitioned into several types according to their sensitivities, and each type of sensitive parameter is estimated in an individual loop by repeated forecast and assimilation. We test this scheme with a synthetic case and a distributed hydrologic model concerning the real case of the Zhanghe river basin in China. The results from the synthetic experiments show that this new scheme can retrieve optimal parameter values and represent the correlations in a more stable manner when compared with the standard state augmentation technique. The real case further demonstrates the robustness of the partitioned update scheme for state and parameter estimation owing to the low estimation errors of streamflow in the assimilation and the prediction periods.

Citation: Xie, X., and D. Zhang (2013), A partitioned update scheme for state-parameter estimation of distributed hydrologic models based on the ensemble Kalman filter, *Water Resour. Res.*, *49*, 7350–7365, doi:10.1002/2012WR012853.

1. Introduction

[2] Hydrologic modeling is always plagued by various uncertainties associated with model parameters, driving force inputs, model structure, and output observations [*Ajami et al*., 2007; *Zhang*, 2002]. To reduce these uncertainties, model calibration that aims to minimize the discrepancy between simulated and observed model outputs is a mandatory element of a good modeling practice [*Refsgaard et al*., 2010]. For many years, a great effort has been directed toward calibration methods, including direct search optimization [e.g., *Duan et al*., 1992, 1993] and probabilistic estimation [e.g., *Beven and Binley*, 1992; *Beven and Freer*, 2001a].

[3] However, most of these methods attribute the underlying uncertainty in the input-output representation of the model to the uncertainty of parameter estimates [*Kavetski et al*., 2004; *Vrugt et al*., 2005]. A few studies based on the Bayesian theorem have tried to account for various sources of uncertainties (e.g., the Bayesian approach for total error analysis (BATEA)) [*Kavetski et al*., 2004], but such approaches are rarely used for nonlinear watershed models [*Vrugt et al*., 2005]. A comprehensive review on confronting modeling uncertainties can be found in *Kavetski et al*. [2004] and *Liu and Gupta* [2007].

[4] In a separate line of research, newly developed data assimilation methods, especially sequential data assimilation techniques, have demonstrated potential for explicitly dealing with various uncertainties and for optimally merging observations into uncertain model predictions [*Troch et al*., 2003]. One of these techniques is the particle filter that is suitable for non-Gaussian nonlinear dynamical models [*Han and Li*, 2008]. Particle filters have received much attention in hydrologic modeling [*DeChant and Moradkhani*, 2012; *Moradkhani et al*., 2005a; *Moradkhani and Sorooshian*, 2008]; however, they may impose a remarkable computational burden for obtaining accurate results [*Weerts and El Serafy*, 2006; *Han and Li*, 2008]. As a prototype of sequential data assimilation techniques, the Kalman filter (KF) [*Kalman*, 1960] and the ensemble Kalman filter (EnKF) [*Evensen*, 1994] recursively result in optimal estimation for linear dynamic models with Gaussian uncertainties. The EnKF has earned its popularity in hydrology due to its attractive features, such as real-time adjustment and ease of implementation [*Reichle et al*., 2002]. In some applications, it was mainly used for dynamic state estimation, while the parameters were fixed at predefined values, thereby explicitly ignoring the effects of parameter uncertainty and interaction [*Vrugt et al*., 2005]. That is partly

[1]State Key Laboratory of Remote Sensing Science, College of Global Change and Earth System Science, Beijing Normal University, Beijing, China.
[2]ERE and SKLTCS, College of Engineering, Peking University, Beijing, China.

Corresponding author: X. Xie, State Key Laboratory of Remote Sensing Science, College of Global Change and Earth System Science, Beijing Normal University, Beijing 100875, China. (xianhong@bnu.edu.cn)

0043-1397/13/10.1002/2012WR012853

attributable to the fact that the parameter estimation is more difficult than the state estimation in hydrology, since the relation between parameters and states are nonlinear for most hydrological models and model parameters cannot be directly measured like states.

[5] The EnKF also provides a general framework for state and parameter estimation. This joint estimation can be performed, typically, with two strategies. One is a hybrid strategy with simultaneous optimization and data assimilation [*Vrugt et al*., 2005]. Its implementation consists of an inner EnKF loop and an outer global-optimization loop. The former is for state estimation conditioned on an assumed parameter set, and the latter for batch estimation of parameters using an optimization method, such as the Shuffled Complex Evolution Metropolis (SCEM-UA) algorithm [*Vrugt et al*., 2003]. The optimal set of parameters identified by this strategy, however, does not guarantee the best model forecasts when the data assimilation is not implemented or no state adjustments are allowed. The other is a state augmentation strategy, which extends the state vector to include the parameter set. Parameters are considered as part of the model state, and they are updated together with the dynamic states when observations are available [*Annan et al*., 2005]. So this technique is a simple extension of the EnKF in which the parameter estimation problem is generally formulated to find the joint probability density of parameters and model states, given a set of measurements and a dynamic model with known uncertainties [*Evensen*, 2009].

[6] For joint state-parameter estimation, the state augmentation technique with the EnKF has been successfully demonstrated in many areas, such as the earth system model [*Annan et al*., 2005], the hydrogeologic model [*Chen and Zhang*, 2006; *Liu et al*., 2008], and catchment-scale hydrologic models [*Young*, 2002; *Xie and Zhang*, 2010]. This technique is also undergoing improvement. One example is the constrained schemes that can be exerted on the EnKF to avoid violating physical principles in updating states and parameters [*Wang et al*., 2009]. Another example is the dual state-parameter estimation approach that can decrease the degree of freedom of the augmented state vector in the updating process [*Moradkhani et al*., 2005a, 2005b]. In addition to the EnKF, particle filtering has also been used for joint state-parameter estimation [*Moradkhani et al*., 2005a, 2005b]. However, most of these applications in rainfall-runoff characterizations aim at lumped hydrologic models with a small number of states and parameters.

[7] For distributed hydrologic models, this state augmentation technique may suffer from spurious or incorrect correlations between states and parameters, which would directly spoil parameter estimation during data assimilation. This is basically due to biased model error quantification and a large degree of freedom for high-dimensional vectors of the augmented state. This disadvantage will be transferred to the covariance matrix that is computed with the (biased) ensemble states within the framework of the EnKF. Especially for the nonlinear impulse response, such as the rainfall-runoff process, the correlations between dynamic states and parameters are easily overestimated or underestimated by the interference of parameters, since different types of parameters contribute differently to the impulse response in the alternate wet-dry seasons. Moreover, when the augmented state vector holds a high dimension, the joint estimation is possibly unstable and intractable [*Moradkhani et al*., 2005a, 2005b]. To better approximate the correlations, a localization scheme is capable of suppressing correlations beyond a certain separation distance [*Reichle and Koster*, 2003]. The localization scheme may be impractical for the joint state-parameter estimation, however, especially since observations (typically, of streamflow) are usually sparse in a watershed.

[8] To reduce the degree of freedom of high-dimensional states and achieve simultaneous state-parameter estimation, a partitioned update scheme based on the EnKF is proposed in this study. This scheme, inspired by the localization scheme [*Reichle and Koster*, 2003] and the dual state-parameter estimation approach [*Moradkhani et al*., 2005a, 2005b], partitions the parameter set according to the parameter types, and estimates the dynamic states and parameters by repeatedly assimilating observations after a separate forecast. Moreover, the parameters are artificially evolved at each time step using a kernel smoothing method to overcome the overdispersion of parameter samples [*Liu*, 2000]. This scheme is first examined with synthetic experiments and further evaluated with a distributed hydrologic model regarding a real case. Results show that this partitioned update scheme can strengthen and expand the robustness of the state augmentation technique due to the fact that it retrieves acceptable parameter values and captures the temporal patterns of dynamic states compared with the standard state augmentation technique. It should be noted that, in this paper, distributed hydrologic models hold a general definition [*Reed et al*., 2004; *Smith et al*., 2004] that includes conceptual distributed models (e.g., the Soil and Water Assessment Tool (SWAT) model used in this study) and fully physically based models [e.g., the SHE model, *Refsgaard et al*., 2010].

[9] The connotation of the parameter type is associated with the distributed hydrologic model in which each computational unit contains the target parameter to be estimated. For example, in SWAT, the parameter CN_2 (see section 4.2) is related to the surface runoff generation in each hydrologic response unit (HRU). Since there are many CN_2 parameters to be estimated for all HRUs in a watershed, "CN_2" is regarded as one parameter type. In a general sense, it is also reasonable that a parameter type contains only one parameter, as shown in section 3, for the synthetic experiments.

[10] This paper is organized as follows. In section 2, we present an overview of the EnKF framework and describe the new parameter update scheme with the kernel smoothing method for parameter evolution. In section 3, we examine the performance of the new algorithm by means of synthetic experiments with a simplified rainfall-runoff model. In section 4, we further demonstrate the scheme using a real case using a distributed hydrologic model, i.e., the SWAT. Finally, in section 5, we summarize the methodology and discuss the results.

2. Data Assimilation Method

2.1. Ensemble Kalman Filter

[11] As a Monte-Carlo variant of KF, the EnKF propagates an ensemble of model realizations to represent the

error covariance of states, projects the states into an observational space, and then updates the prior ensemble with a linear combination of the modeling and the observation [*Evensen*, 1994]. The EnKF operates sequentially by performing, in turn, a forecast step and then a filter update step. In general, the forecast step for an ensemble member i between times t and $t-1$ can be written as:

$$x_t^{i-} = M\left(x_{t-1}^{i+}, \theta, u_t^i\right) + e_t^i, \quad e_t^i \sim N(0, Q_t) \tag{1}$$

where x_t^{i-} and x_{t-1}^{i+} are the forecast state vector at time t and the updated state vector at time $t-1$, respectively; $M(\cdot)$ stands for a nonlinear model operator; θ is the model parameter vector and is assumed to be known; and u_t^i is the forcing input vector. The model error vector e_t^i (or perturbation vector) is assumed to obey Gaussian distribution with zero means and covariance Q_t.

[12] Based on a linear correction, the filter update step at time t can be expressed as:

$$x_t^{i+} = x_t^{i-} + K_t\left(y_t^i - H(x_t^{i-}, \theta)\right) \tag{2}$$

where y_t^i denotes the ith observation sample obtained by adding a Gaussian noise to the actual observation; and H is the observation operator that maps the model states to the observation space. For detailed computation of the Kalman gain matrix, K_t, please refer to *Evensen* [2003].

[13] For the joint parameter and state estimation, the state vector x_t can be augmented to include the parameter vector θ, which is perturbed initially based on a priori distribution. As the model ensemble evolves, the parameter vector is passively updated together with state variables when observations are available. A brief description about this standard joint parameter and state estimation is given in section 2.3.2. We will focus on the discussion of the improvement based on this standard augmentation technique.

2.2. Parameter Evolution

[14] In the framework of joint estimation, the ensemble of parameters is prone to shrink with the ensemble of parameters being updated in data assimilation (i.e., the variance of parameters will become small). Thus, the parameter evolution is often needed to avoid ensemble shrinkage and filter degeneracy [*Liu*, 2000], although this idea may violate, to some degree, the basic conception that the parameters are principally assumed to be constant in dynamic models. Correspondingly, we would expect the rate of the parameter variations to be slower than that of the state variation [*Liu and Gupta*, 2007]. One of the ideas considers the parameter evolution as a random walk process by adding small random perturbations to the *posterior* distribution at each time step:

$$\theta_t^{i-} = \theta_{t-1}^{i+} + \tau_t^i, \quad \tau_t^i \sim N(0, T_t) \tag{3}$$

where θ_t^{i-} is the ith ensemble member forecast at time t; θ_{t-1}^{i+} is the ith updated ensemble member at time $t-1$; $\overline{\theta}_{t-1}^{+}$ is the ensemble mean of the n members; and T_t is a predefined covariance. This idea has been used in many cases [e.g., *Chen and Zhang*, 2006; *Wang et al*., 2009], but it contains a key drawback in that such perturbations will cause overdispersion of parameter samples, loss of information between time steps, and a diffused posterior spread of parameters [*Liu*, 2000; *Moradkhani et al*., 2005a, 2005b].

[15] One remedy for this problem is the kernel smoothing of parameter samples, developed by *West* [1993] and extended by *Liu* [2000]. It can be briefly expressed as:

$$\theta_t^{i-} = \alpha\theta_{t-1}^{i+} + (1-\alpha)\overline{\theta}_{t-1}^{+} + \tau_t^i, \quad \tau_t^i \sim N(0, T_t) \tag{4}$$

$$\overline{\theta}_{t-1}^{+} = \frac{1}{n}\sum_{i=1}^{n}\theta_{t-1}^{i+} \tag{5}$$

$$T_t = h^2 \mathrm{var}\left(\theta_{t-1}^{+}\right) \tag{6}$$

where α is the shrinkage factor being restricted in (0, 1], typically in [0.95, 0.99], h is the smoothing factor with a relation of $\alpha^2 + h^2 = 1$ and T_t is the covariance derived from the smoothing factor and the ensemble variance var $\left(\theta_t^{+}\right)$. In this method, only one variable, the smoothing factor h, is to be determined experimentally and somewhat subjectively. Moreover, it may depend on the magnitude of the ensemble variance var $\left(\theta_{t-1}^{+}\right)$. When var $\left(\theta_{t-1}^{+}\right)$ is quite large, h will be defined as $\sqrt{1-\alpha^2}$ to reduce the ensemble spread. When var $\left(\theta_{t-1}^{+}\right)$ is so small that it may eventually cause filter divergence, h needs to be specified with a larger value $(h > \sqrt{1-\alpha^2})$ to inflate the ensemble spread ($h = 1.0$ in this study).

[16] Clearly, the overdispersion issue is relaxed by the location shrinkage, which pushes samples θ_{t-1}^{+} toward their mean $\overline{\theta}_{t-1}^{+}$ before adding a small perturbation implied in the normal kernel. The parameter vector after this evolution (i.e., θ_t^{-}) is increasingly randomized to some degree due to the added random numbers (i.e., τ_i in equation (4)). The magnitude of this randomization (i.e., T_t in equation (6)) is greater than the variance of the initial ensemble spread (equal to $((1-\alpha)^2 \mathrm{var}\left(\theta_{t-1}^{+}\right)$, derived from the variance of the $1-\alpha$ times of anomalies of parameters). However, the ensemble mean and variance are preserved in parameter evolutions, providing a smooth density between time t and time $t-1$. So this artificial evolution offers the advantage of the random walk scheme to avoid the ensemble shrinkage, while constraining discontinuity in parameter evolutions and information loss over time. It has been successfully applied for parameter estimation in hydrologic models [*Moradkhani et al*., 2005a, 2005b] and ecosystem models [*Chen et al*., 2008]. In this study, we incorporate it into the data assimilation algorithms to evolve the parameters, unless otherwise mentioned.

2.3. Methodology of Parameter Updating

2.3.1. Partitioned Update Scheme

[17] In the standard joint state-augmentation method (called SU_EnKF hereafter), the covariance approximation with a limited ensemble size and perturbed noises is likely to yield an erroneous covariance due to the nonlinear relations between states and parameters [*Moradkhani et al*., 2005a, 2005b]. With such covariance in the Kalman gain matrix, consequently, the simultaneous update of states and parameters is likely to be impaired (e.g., unstable estimation). Although the nonlinearity is model-dependent, a

general character of hydrological models is the impulse response of rainfall-runoff. Thus, some model parameters are activated or inactivated periodically. For example, the parameter associated with surface runoff (e.g., CN_2 in SWAT) is only activated when rainfall occurs. During non-rainfall periods, (in the dry season, the groundwater flow is dominant), if all parameters are updated based on equations (6) and (7), unstable or unreasonable estimations may be obtained because of the parameter interference in nonlinear models [*Moradkhani et al*., 2005a, 2005b]. Hence, the SU_EnKF should be used prudently [*Moradkhani et al*., 2005a, 2005b; *Young*, 2002].

[18] To better approximate the covariance between states and parameters, here we propose a partitioned update scheme (called PU_EnKF hereafter). This scheme partitions the parameters into several types according to their sensitivities, and each type of parameter is updated separately within m loops (here m is the number of parameters or the number of parameter types to be estimated). A flowchart of this scheme is provided in Figure 1. After the states and parameters are initialized, the mean of each parameter is calculated with equation (4), and then the procedure goes into loops of joint estimation. In each loop, the state is forecasted using equation (1), but conditioned only on one target type of parameter (evolved with the kernel smoothing method, equations (3–5)) while the other parameters are prescribed with their means. Specifically, the parameter vector $(\lambda_{j,t}^{i})$ has three parts: The first is the means of the newly updated parameters from the prior loops at the current time step t; the second is the target type of parameter to be updated at the current loop; and the third is the means of the parameters estimated at the previous time step $t-1$. The forecast error covariance P_t and the Kalman gain K_t are computed based on the evolved parameters and all dynamic states. Subsequently, the target type of parameter is appended into the state vector and all parameters in this type are jointly updated. Through the m loops, all types of parameters are estimated along with m ensembles of states. The optimal estimate of each state can be approximated by the average of all the members from the m ensembles.

[19] Note that, when the parameters exhibit spatial variability represented in computational units or grids (e.g., the curve number (CN_2) in the SWAT model), the number of loops (m) can be set as the number of parameter types to be estimated instead of the number of parameters, and each type contains a number of parameters corresponding to the computational units. In total, there are $m \times n$ model runs, since each of the m loops employs n model runs that correspond to the current target type of parameters. Accordingly, there are $m \times n$ realizations for dynamic states, but n realizations for the parameters. The group of n realizations for one type of parameters is regarded as a subensemble.

2.3.2. Comparison of PU_EnKF and SU_EnKF

[20] To further distinguish the advantages of PU_EnKF, we explain the difference between PU_EnKF and SU_EnKF in theory and in implementation. For simplicity, equation (1) is assumed to have a state variable (x) and two parameters (θ_1, θ_2): $x_t = M(x_{t-1}, \theta_1, \theta_2)$. The observation operator is also simplified as $H = [1, 0]$ for PU_EnKF and $H = [1, 0, 0]$ for SU_EnKF.

[21] As mentioned in section 2.1, the forecast step within SU_EnKF is expressed as:

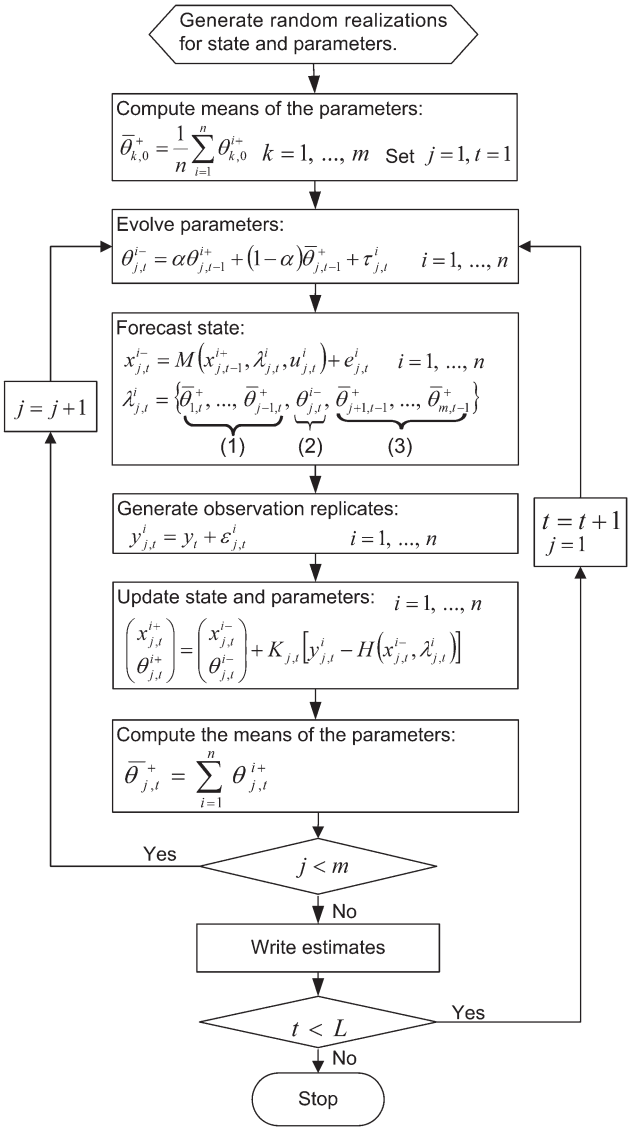

Figure 1. Flowchart of the PU_EnKF (n is the subensemble size; m is the number of parameters or the number of types of parameters to be estimated; L is the length of the time period; and the other symbols are explained in the text).

$$x_t^{i-} = M\left(x_{t-1}^{i+}, \theta_{1,t}^{i-}, \theta_{2,t}^{i-}\right) + e_t^{i}, i = 1, ..., N \tag{7}$$

[22] Then, the Kalman gain matrix is written as:

$$K_t = \begin{bmatrix} \mathrm{cov}\,(X_t^-, X_t^-) \\ \mathrm{cov}\,(X_t^-, \theta_{1,t}^-) \\ \mathrm{cov}\,(X_t^-, \theta_{2,t}^-) \end{bmatrix} \frac{1}{\mathrm{cov}\,(X_t^-, X_t^-) + R_t} \tag{8}$$

where N is the ensemble size; $\mathrm{cov}(\cdot)$ denotes the covariance that is computed from the ensemble of the state (i.e., X_t^-) and of the two parameters (i.e., $\theta_{1,t}^-$ and $\theta_{2,t}^-$); and R_t is the measurement error covariance.

[23] For the PU_EnKF scheme, according to the framework in Figure 1, the state-parameter estimation procedures

are conducted by two iterative loops with respect to the two parameters. For θ_1 estimation, the forecast step is:

$$x_{1,t}^{i-}=M\left(x_{1,t-1}^{i+},\theta_{1,t}^{i-},\overline{\theta_{2,t-1}^{+}}\right)+e_t^i,\quad \text{i}=1,\ \div,\ \text{N} \tag{9}$$

[24] And the associated Kalman gain matrix is written as:

$$K_{1,t}=\begin{bmatrix}\text{cov}\,(X_{1,t}^{-},X_{1,t}^{-})\\ \text{cov}\,(X_{1,t}^{-},\theta_{1,t}^{-})\end{bmatrix}\frac{1}{\text{cov}\,(X_{1,t}^{-},X_{1,t}^{-})+R_t} \tag{10}$$

[25] The new estimate of θ_1, with this Kalman matrix, can be obtained at the update step similar to equation (2), and its updated ensemble mean $\overline{\theta_{1,t}^{+}}$ is used in the second loop for θ_2 estimation:

$$x_{2,t}^{i-}=M\left(x_{2,t-1}^{i+},\overline{\theta_{1,t}^{+}},\theta_{2,t}^{i-}\right)+e_t^i,\quad i=1,...,N \tag{11}$$

$$K_{2,t}=\begin{bmatrix}\text{cov}\,(X_{2,t}^{-},X_{2,t}^{-})\\ \text{cov}\,(X_{2,t}^{-},\theta_{2,t}^{-})\end{bmatrix}\frac{1}{\text{cov}\,(X_{2,t}^{-},X_{2,t}^{-})+R_t} \tag{12}$$

[26] So there are quite a few differences in the state forecast and the Kalman matrix computation between SU_EnKF and PU_EnKF. In SU_EnKF, the state forecast is conditioned on all parameters, and the covariances in equation (7), computed from the ensembles of state and parameters, are prone to contamination. In PU_EnKF, however, the state forecast is conditioned on the target parameter. An iterative manner is employed to update each parameter and, thereby, pushes the estimates of the parameters toward optimal values. Moreover, this will reduce the degree of freedom, diminish interference from different types of parameters, and is expected to achieve a more accurate representation of the covariances between parameters and dynamic states.

[27] Note that this partitioned update scheme may be sensitive to the updating order of parameter types. We will present a short discussion in section 3 of the synthetic experiments. Moreover, it probably has high-computational costs due to the m loops; this is especially the case when it is used in a complex physical system that consists of a large number of parameter types to be estimated, such as distributed hydrologic modeling. To mitigate this issue, the number of loops can be compressed by updating the sensitive types of parameters while the other insensitive ones are prescribed with prior knowledge. So a sensitivity analysis should be performed beforehand for a large system to identify the most sensitive types of parameters. On the other hand, the computational cost of this partitioned update scheme is still lower than that of the standard state-augmentation algorithm specified with ensemble size $m \times n$.

3. Evaluation Using Synthetic Experiments

[28] Synthetic experiments are used to test the performance of the PU_EnKF and to compare it with the SU_EnKF. The following experiments associated with the SU_EnKF are deliberately prescribed with a large ensemble size ($m \times n$, as indicated in Figure 1), unless stated otherwise. This is based on the consideration that the large ensemble size could render better state and parameter estimation due to the Monte-Carlo nature of the EnKF. Both schemes employ the same parameter evolution algorithm in this study, i.e., the kernel smoothing method. Moreover, the comparison of the two schemes is done with an equal number of model runs ($m \times n$).

[29] The synthetic experiments involve a simplified rainfall-runoff model. They are implemented in two steps. First, a reference simulation with the model is conducted based on a known set of parameters. The outputs from the simulation then serve as the "truth," which is used to generate observations. Second, the assimilation experiments are performed with erroneous initial parameters. The results of assimilation estimates are compared against the true state and the known parameters.

3.1. A Simplified Rainfall-Runoff Model

[30] A simplified rainfall-runoff model is used that concerns the surface runoff process exclusively. The runoff generation is represented with the Soil Conservation Service (SCS) model [*Ponce et al*., 1996; *Rallison and Miller*, 1981], and the runoff concentration is characterized with an exponential function. This model has been widely implemented in hydrologic models, such as SWAT [*Neitsch et al*., 2001] that will be depicted in section 4. For a basin of interest, the generated surface runoff and the amount of water released into a main channel are expressed as:

$$Q_{total,k}=Q_{surf,k}+Q_{bf,k} \tag{13}$$

$$Q_{surf,k}=\left(Q_k+Q_{st,k-1}\right)\left[1-\exp\left(\frac{-surlag}{t_{conc}}\right)\right] \tag{14}$$

$$Q_{st,k}=Q_k+Q_{st,k-1}-Q_{surf,k} \tag{15}$$

$$Q_k=\frac{(R_k-0.2S)^2}{R_k+0.8S} \tag{16}$$

$$S=\frac{25400}{CN}-254 \tag{17}$$

where $Q_{total,k}$ is the total runoff released to the main channel, consisting of the surface flow $Q_{surf,k}$ and the base flow $Q_{bf,k}$; $Q_{st,k}$ is the stored or lagged surface runoff; *surlag* is the surface runoff lag coefficient; t_{conc} is the time of concentration for the basin; Q_k is the generated surface runoff on recent day k; R_k is the rainfall depth for the day; and S is the retention parameter determined by the curve number *CN*. The surface runoff (calculated with equation (16)) only occurs when $R_k > 0.2S$. In general, the curve number *CN* is constrained between 30 and 100.

3.2. Assimilation Setup and Results

[31] In order to further simplify this synthetic experiment, we focus on only two parameters, *surlag* and *CN*, because the two are quite sensitive to the rainfall-runoff relationships. Moreover, the time of concentration is set as $t_{conc}=16.0$h, and the base flow is specified with a constant value $Q_{bf,k}=5.0$. So the total runoff can be simply written as $Q_{total,k}=f(Q_{st,k-1},R_k,surlag,CN)$, in which the rainfall R_k as a driving force is from measurement records. Thus, the runoff process is a nonlinear response to the driving force of rainfall. Figure 2 (top) plots a typical response,

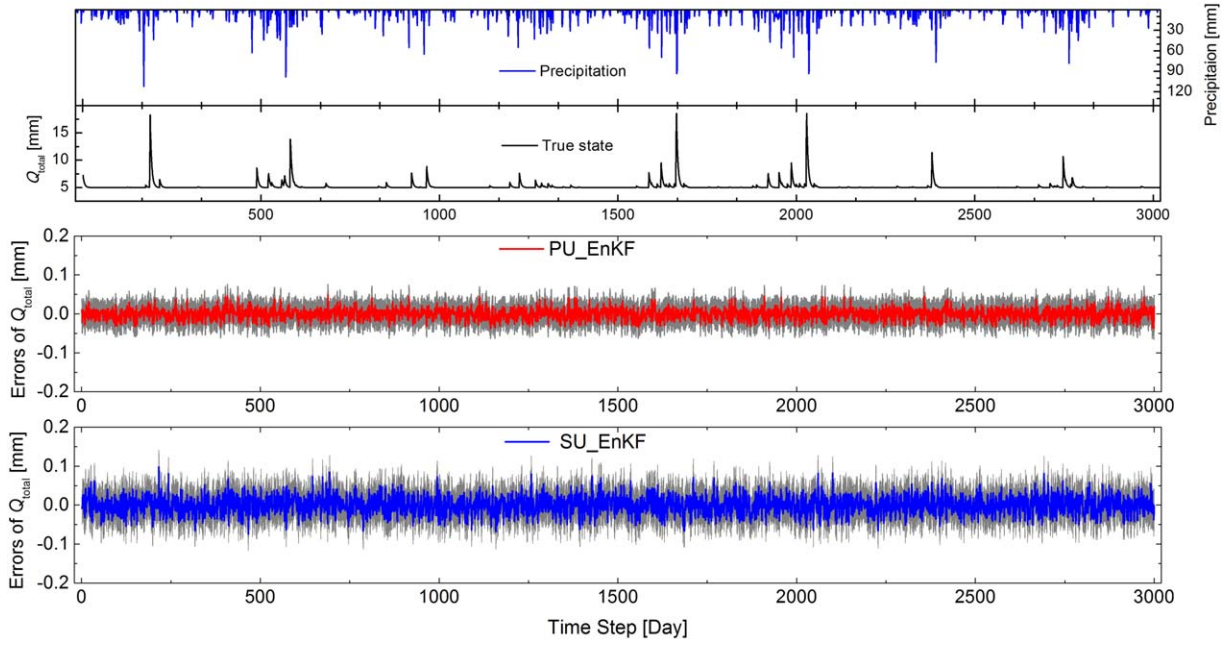

Figure 2. The precipitation and the corresponding true runoff series, and the estimation errors of runoff from the two assimilation schemes. The gray shaded areas correspond to 95 percentile confidence intervals.

which is produced by the reference simulation given a set of parameter values (Table 1).

[32] In the PU_EnKF assimilation, we adopt three update loops ($m = 3$) to include an individual update for the state ($Q_{st,k}$ and $Q_{total,k}$) because of the simplicity of the equation and affordable computational cost. The subensemble size is $n = 80$ within each update loop, and the parameter estimation order is {*CN*, *surlag*}. Accordingly, the ensemble size for the SU_EnKF assimilation is prescribed as 240 ($m \times n = 240$). As mentioned before, the storage space in the SU_EnKF is much larger than that in the PU_EnKF for this treatment. The smoothing factor for the two schemes (equation (3)) is set as $\alpha = 0.99$ and $h = \sqrt{1-\alpha^2}$, empirically. The ensemble spread is inflated by $h = 1.0$ if the standard variance of parameters is smaller than 0.05 times the predefined width (Table 1). The estimation error of the state is calculated using the mean of the ensemble minus the true values. The root mean square error (RMSE) and the mean absolute error (MAE) are computed with respect to the last 2500-step estimates of total runoff. The other setups are exhibited in Table 1. Although the initial realizations of parameters are obviously biased compared to the true values in this synthetic case, please note that parameter bias is not necessary for the PU_EnKF or the SU_EnKF.

[33] Figure 2 plots the state estimation errors. The PU_EnKF scheme renders relatively small errors compared to the SU_EnKF. This fact is also indicated by the smaller RMSE and MAE, shown in Table 1. Moreover, the PU_EnKF scheme provides desirable estimations for both parameters that approach true values; whereas, the SU_EnKF scheme gives unstable estimations for the parameter *CN* (Figure 3). In the parameter estimation process, the two assimilation schemes adjust the model parameter estimates as a response to the peak-runoff occurrences, such as at the 200th and the 520th time step. However, the magnitude of adjustment is different within the two assimilation schemes because of the difference in the representation of the state-parameter covariances.

[34] For the SCS model, as expressed within equations (6–10), the generated surface runoff positively relates to the two parameters, especially with strong correlation to the parameter *CN*, similar to the SWAT model taking the parameter CN_2 as a dominant parameter in surface runoff generation [*Neitsch et al*., 2001; *Holvoet et al*., 2005]. This

Table 1. Reference and Assimilation Setups and the Assimilated Results[a]

	Initial Setting			Noise Variance		Final Estimates			
Integrations	*CN*	*Surlag*	$Q_{st,0}$	*Q*	*R*	*CN*	*surlag*	RMSE of Q_{total}	MAE of Q_{total}
Reference	75.0	4.0	10.0						
PU_EnKF	*U*(65.0, 98.5)	*U*(0.1, 13.0)	$N(4.0, 6.0^2)$	2.0	0.2	$(74.56, 1.55^2)$	$(3.51, 0.93^2)$	0.014	0.011
SU_EnKF	*U*(65.0, 98.5)	*U*(0.1, 13.0)	$N(4.0, 6.0^2)$	2.0	0.2	$(72.07, 2.01^2)$	$(4.23, 0.84^2)$	0.023	0.018

[a] *Q* and *R* are the noise variances for modeling and observations; final estimates of parameters are represented with means and variances in the brackets; and RMSE and MAE denote the root mean square error and the mean absolute error of the 800-step estimates of *X*, respectively. *U* and *N* indicate the uniform and normal distribution, respectively.

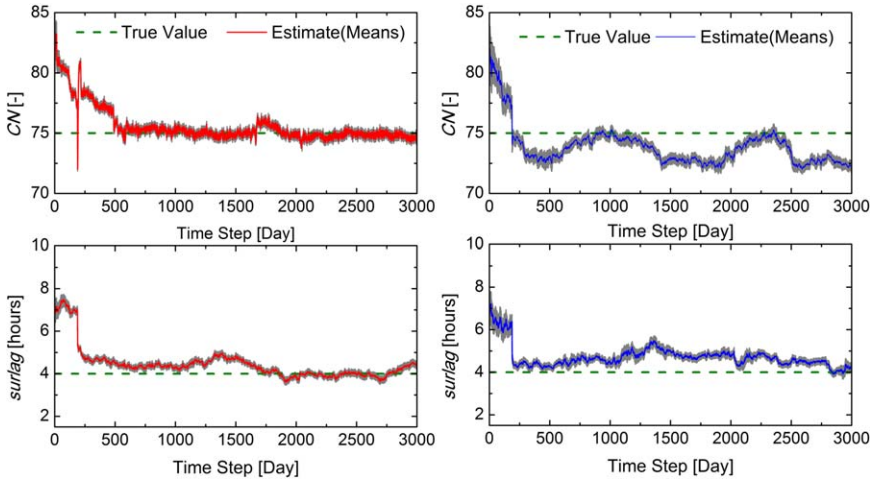

Figure 3. Estimation processes of parameters in the simplified rainfall-runoff model using the two assimilation schemes: (left) the PU_EnKF and the (right) SU_EnKF. The gray shaded areas correspond to 95 percentile confidence intervals.

property is reasonably characterized by the PU_EnKF. As shown in Figure 4, in the PU_EnKF experiment, the correlation coefficient between the Q_{total} and the parameter *CN* is around 0.68 after 200 steps, and the correlation coefficient between the Q_{total} and the parameter *surlag* is always positive with an average of 0.05. In contrast, the SU_EnKF renders negative correlations in some periods, with averages around zero, for the Q_{total} with the two parameters. Thus, the SU_EnKF exhibits inconsistent and spurious correlations with respect to model formulation. This inconsistency stems from the parameter interference when the two parameters are added to the state vector and updated simultaneously. However, the PU_EnKF can mitigate this issue owing to its partitioned update scheme for model parameters.

3.3. Verification of the Partitioned Iteration Update Scheme

[35] There is a concern that the advantage of PU_EnKF might come from its three times of data assimilation, not from its partitioned iteration scheme, thereby reducing the parameter biases. To verify such an advantage of the PU_EnKF, we intentionally design two scenarios based on the SU_EnKF scheme instead of the PU_EnKF scheme.

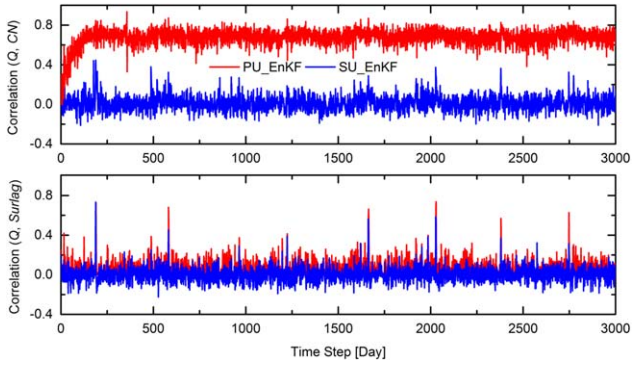

Figure 4. Correlation coefficients between the total runoff (Q_{total}) and the two parameters (*surlag* and *CN*).

One is a multiassimilation scheme in which the observation information is assimilated m times (here $m = 3$) at each time step, and all states and parameters jointly undergo the forecast and the update steps in an iterative manner. The only difference between this multiassimilation scheme and the PU_EnKF scheme is that the former updates all parameters and states jointly, similar to that done in SU_EnKF, but the latter forecasts the state and updates each parameter separately. The other scenario adopts a spin-up scheme for data assimilation. The forecast-update procedures using the SU_EnKF scheme are run through the entire period (3000 days in this study) for m times, while the parameter estimates at the end of the previous data assimilation are used to initiate the next data assimilation. In this scenario, the initial biases of parameters are expected to be reduced. For a fair comparison, the same number of ensemble members is used in those scenarios as in the PU_EnKF experiment, i.e., $n = 80$.

[36] Figure 5 shows the results from the multiassimilation scheme. The trajectories of parameter estimations fluctuate around the true values of parameters. The parameter *CN* estimation is not acceptable due to the difference from its true value. It is even not as acceptable as the SU_EnKF scheme with large ensemble size (right column of Figure 3). Figure 6 shows the parameter estimation from the spin-up assimilation scheme. The final spin-up estimations with the SU_EnKF present better estimates than the first. Actually, the third spin-up estimation shows similar trajectories to the second (not shown) with a small improvement; whereas, there is no notable improvement for the state estimation in the final assimilation (not shown) relative to the data assimilation with a large ensemble size (i.e., 240) but without spin-up (Figure 2).

[37] Therefore, the multiassimilation scheme fails to achieve the true or the optimal values of parameters. Moreover, updating all parameters repeatedly m times at each assimilation step is not a good strategy for parameter estimation in hydrological models partly due to the parameter interference, as stated in section 2.3. The capability of the SU_EnKF scheme for state and parameter estimation is

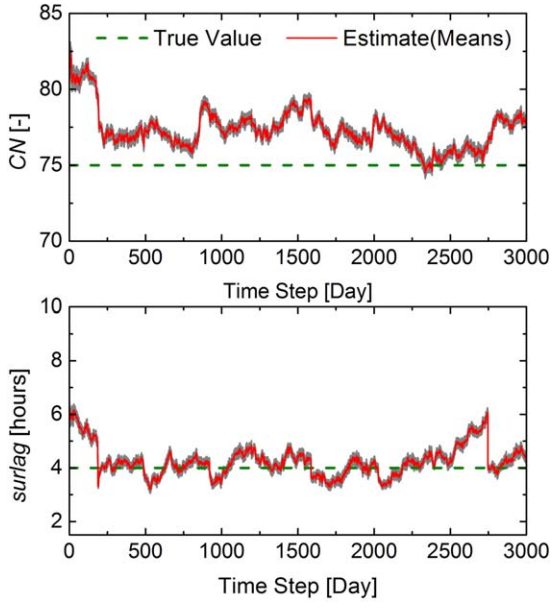

Figure 5. Parameter estimation using the multiassimilation scheme: all parameters and states are updated three times at each time step. The gray shaded areas correspond to 95 percentile confidence intervals.

limited even with spin-ups to reduce the initial biases of parameters. On the other hand, these scenarios demonstrate that the effectiveness of the PU_EnKF scheme stems from its partitioned iteration scheme, and that the initial biases of parameters may not be influential in the data assimilation performance.

3.4. Effect of the Parameter Evolution Algorithm

[38] The performance of state-parameter estimation would be impacted by the parameter evolution algorithm. To examine the effect of parameter evolution, i.e., the kernel smoothing, we designed a scenario by removing the kernel smoothing in the PU_EnKF scheme. The parameters are updated along with the state variable. Moreover, we defined the other scenario in which the parameters are evolved using the random walk process (equation (3)). In this parameter evolution algorithm, zero-mean Gaussian random perturbations are added to the parameters after the assimilation update, and their standard variances are set as 2.0 and 0.2 for *CN* and *surlag*, respectively.

[39] Figure 7 shows the results from the above two scenarios. When the kernel smoothing is removed, the ensemble spreads (indicated by the confidence interval) of parameters quickly shrink, and there is no obvious improvement for parameter estimation even after the 190th assimilation time step. The estimations for the two parameters do not capture their true values. When the random walk evolution of parameters is used, however, the estimates of parameters approximately agree with the true values, especially for the parameter *CN*; for *surlag*, the estimates fluctuate with the assimilation processes.

[40] Therefore, the PU_EnKF without parameter evolution presents an unfavorable situation due to the ensemble spread shrinkage. If the ensemble spread shrinkage occurs, the estimates of parameters cannot be improved and be reactivated from a suboptimal value. Random walk evolution is a better alternative by perturbing the ensemble, though it causes discontinuities in parameters and the loss of information. A comparison with the previous results shown in Figure 3 indicates that the parameter evolution with the kernel smoothing performs best among the three for parameter estimation within the PU_EnKF; this is because a small perturbation is employed in the kernel smoothing while the ensemble mean and variance are preserved. The discontinuity caused by such a small perturbation is constrained within a reasonable range by adjusting the parameter α. So this kernel smoothing is a compromise algorithm for parameter evolution. We also implemented the random perturbations for parameters in the SU_EnKF scheme. The results (not shown) are either better or worse than those from the kernel smoothing algorithm, but they are not as good as those from the PU_EnKF. Hence, the combination of this evolution algorithm with the PU_EnKF is a preferable strategy for state-parameter estimation.

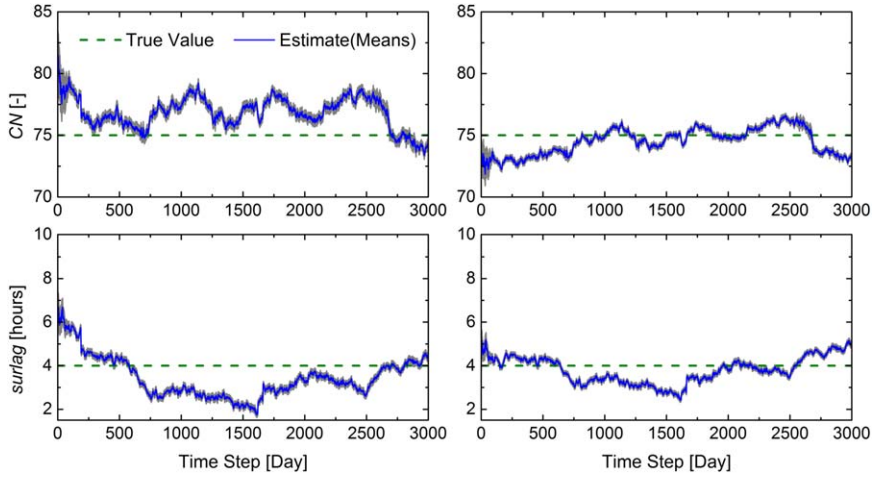

Figure 6. Parameter estimation using the SU_EnKF with three runs of spin-up data assimilation. Only (left) the first and (right) the third spin-up estimations are shown. The gray shaded areas correspond to 95 percentile confidence intervals.

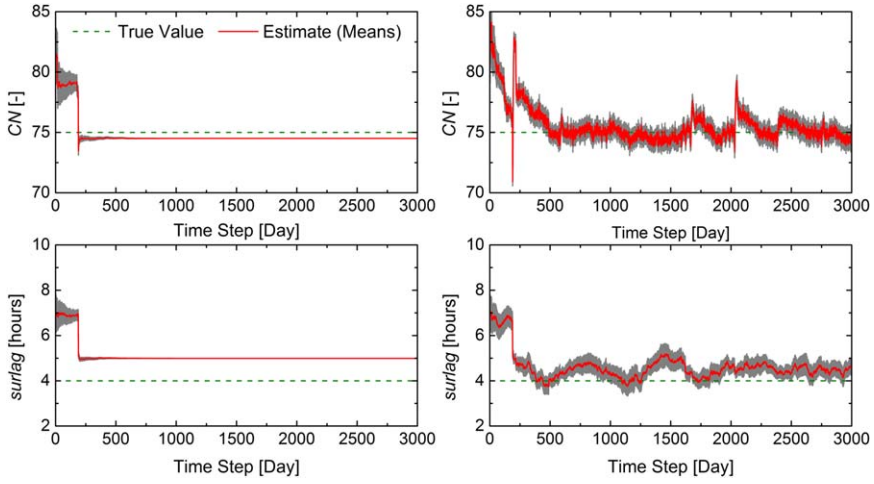

Figure 7. Results from the PU_EnKF without kernel smoothing (left) and with random walk evolution (right) for parameters *CN* and *surlag*. The gray shaded areas correspond to 95 percentile confidence intervals.

3.5. Ordering Effect of Parameter Estimation

[41] The order of parameter estimation in updating loops may influence the performance of data assimilation due to the iterative manner in the partitioned update scheme. Here we present a brief discussion of this problem. The order of the two parameters is exchanged, i.e., {*surlag*, *CN*}, to analyze the ordering effect.

[42] As shown in Figure 8, the PU_EnKF with different parameter-estimation orders also yields acceptable parameter estimates, indicating the robustness of the PU_EnKF. The assimilation in this adjusted order provides a better estimation than did the previous ordering (Figure 8 versus Figure 3), especially for the *CN* estimation. The possible reason for this improvement is that the correct estimate of the less-sensitive parameter (i.e., the *surlag*), obtained from the previous update, will facilitate the estimation of sensitive parameters (i.e., the *CN*). So in separate update loops of the PU_EnKF, it is preferable to update parameters in order of increasing sensitivity. This could be regarded as a general suggestion instead of a strictly validated conclusion as the ordering effect may be problem-dependent.

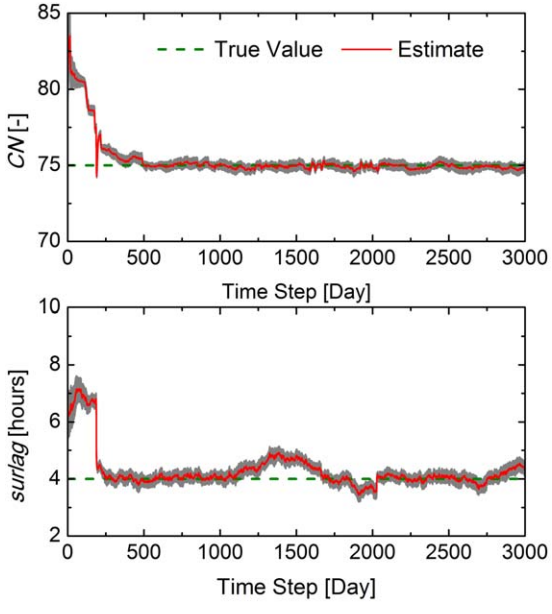

Figure 8. Parameter estimation processes using the PU_EnKF scheme after adjusting the estimation order. The gray shaded areas correspond to 95 percentile confidence intervals.

4. Evaluation Using a Distributed Hydrologic Model

[43] We couple the PU_EnKF with the SWAT model and apply this assimilation system to characterize the rainfall-runoff process of a real basin. We focus on the streamflow estimation on account of data availability. In addition to comparing the results from the data assimilation period, the estimated parameters are further validated for hydrologic prediction using a single model run.

4.1. Study Area and Data Availability

[44] The Zhanghe river basin is an agricultural irrigation area in Hubei Province, China (Figure 9). It covers about 1129 km^2, of which the cultivated area accounts for 59%, followed by forest (16%), bare land (10%), water bodies (9%), and urban areas (6%). Intense human activities including cultivation, irrigation, and drainage make water-cycle representation difficult and present large uncertainties for hydrologic modeling.

[45] Daily streamflow time series, from the years 2003 to 2006, are available from four gauges, marked as A, B, C, and D; gauge D is at the outlet of the basin (Figure 9). Five daily precipitation series from the period of 2002 to 2006 are used. Moreover, daily temperature, radiation, wind speed, and relative humidity from January 2002 to December 2006 are obtained from the Tuanlin Experiment Station. Land-use data with a resolution of 14.25 m were derived from remote-sensing data (Landsat ETM+) [*Cai*, 2007]. Moreover, the soil map with soil properties was obtained from the local agriculture department. Although the prior

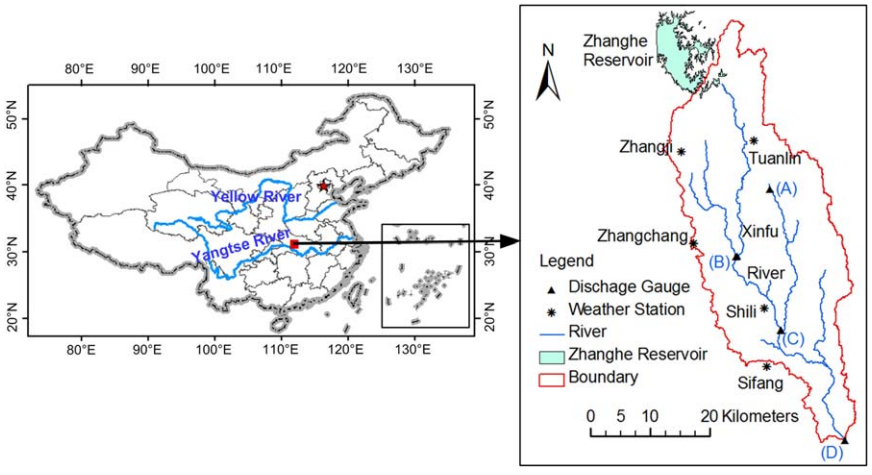

Figure 9. (right) Zhanghe river basin, located in (left) central China.

(default) values of model parameters are derived from the land use and the soil map, they should be further calibrated.

4.2. Distributed Hydrologic Model: SWAT

[46] SWAT is a basin-scale distributed hydrologic model originally developed by the USDA Agricultural Research Service [*Arnold et al*., 1993]. For modeling purposes, a basin is partitioned into multiple subbasins, which are then further divided into hydrologic response units (HRUs) that consist of unique land cover, management, and soil characteristics [*Gassman et al*., 2007; *Neitsch et al*., 2001]. The HRUs are the basic computational units in the SWAT simulation.

[47] We select seven dominant parameters to be estimated in data assimilation according to sensitivity analysis studies for SWAT [*Holvoet et al*., 2005; *Muleta and Nicklow*, 2005; *van Griensven et al*., 2006]. Their default ranges are determined in terms of the lookup tables [*Neitsch et al*., 2001] corresponding to the specific soil and land-use properties of the Zhanghe basin. In addition to these types of parameters, 10 hydrologic variables that underpin the model run are selected to be updated in data assimilation. The first nine variables (Table 3) are the dynamic states that characterize the hydrologic storage status in an HRU or a subbasin, and they will partially influence the next-day hydrologic outputs, i.e., the evapotranspiration (ET) in a subbasin and the streamflow in a river channel (Qr).

[48] Based on the topography, land-use and soil types, the Zhanghe river basin is divided into 20 subbasins and 98 HRUs. The soil column is discretized into four layers with different soil properties. To reduce the number of parameters associated with the four layers, the available water capacity (SOL_AWC) of the soil is assumed to be homogenous. Consequently, there are 606 parameters in total to be estimated, and 954 variables to be updated along with data assimilation. For the SU_EnKF assimilation scheme, the extended state vector consists of 1560 members. For the PU_EnKF, the extended sate vector contains 954 hydrologic variables and 98 or 18 parameters for each type. The number of loops is $m = 7$, corresponding to the selected parameters in Table 3.

4.3. Assimilation Setup

[49] The data assimilation procedures are conducted in three successive steps. First, a well-fed model, prescribed with default parameter values, is warmed up within a period to initialize the model states. Second, at the start of this period, the seven types of parameters for each HRU or subbasin are perturbed to obtain an ensemble of samples, and then these samples are used for ensemble simulations given perturbed precipitation. This is referred to as the "perturbation period" in order to achieve a broad and consistent distribution of the model states, which roughly characterizes state uncertainties. The parameter samples, assumed to be independent and Gaussian, are generated using the Latin hypercube method [*Helton and Davis*, 2003; *Pebesma and Heuvelink*, 1999]. The Gaussian distribution is used because of prior calibration with initially guessed values in *Xie and Cui* [2011]. The standard deviations are constrained to ensure that random samples are within their respective ranges in Table 3. Third, after the two preprocessing periods, the data assimilation period begins, in which the observations are assimilated and the modeling states are updated. In this study, the three steps are activated with 3 year data, from 1 January 2003 to 31 December 2005. The first two steps are used for warming-up the model, and perturbing ensemble simulations are performed for the year 2003, each lasting for half of a year (182 days for warming-up and 183 days for perturbation). The subsequent data assimilation proceeds for 2 years, from 2004 to 2005, to obtain optimal values of the model parameters.

[50] To mimic the uncertainties or errors of model inputs, states and observations, additive perturbations with Gaussian zero-mean are adopted. The standard deviations of the precipitation and the streamflow observations are scaled according to their magnitudes with predefined scale factors, and the standard deviations of two model outputs (i.e., the Qr and SW in Table 3) are scaled to the ensemble means from the SWAT modeling. However, the other eight state variables in Table 3 are assumed to be free of model errors, since these variables are estimated internally and are difficult to prescribe with reasonable errors, and their uncertainties are indirectly reflected in the soil water. Therefore, there are four scale factors to be set concerning the input-forcing (i.e., the precipitation), observed streamflow, the modeling soil water (SW), and streamflow (Qr). Various combinations of factor values are evaluated by

running the two data assimilation schemes from an experiential and practical perspective. Consequently, the factor for input-forcing is set at 0.2, and the observed streamflow is specified at 0.08. The factors for the modeling soil water (SW) and streamflow are set at 0.2. An overestimation of uncertainties is preferable over an underestimation in order to avoid the problem of converging to an incorrect solution [*Clark et al*., 2008; *Crow and Van Loon*, 2006]. Note that the uncertainty representation is still a great challenge in data assimilation, and approaches are emerging that are worth considering, such as adaptive filtering techniques [*Crow and Reichle*, 2008; *Reichle et al*., 2008].

[51] Since only four sites of observed streamflow are available to update the states and parameters of 20 subbasins and 97 HRUs, spurious correlations between states and parameters probably occur due to long distances and impair the performance of data assimilation. To remedy this issue, the covariance localization technique [*Reichle and Koster*, 2003] is used to suppress correlations beyond a certain distance. The basin is divided into four subregions based on the subbasin distribution (Figure 10), and the states and parameters within each region are updated by assimilating streamflow observations from the associated gauge. It is important to mention that runoff and streamflow move through land surface and rivers, from the upper subbasins/rivers to the lower ones, so the observations at a station usually correlate with the states and parameters within its upper subbasins and rivers. Therefore, the observation is used to update the upper and the nearby subbasins. The states and parameters from different subregions are assumed to be uncorrelated for localization.

[52] For the PU_EnKF assimilation, the order of parameter estimation is arranged as {ESCO, *surlag*, GWQMN, ALPHA_BF, CH_K, SOL_AWC, CN_2}, in which the most sensitive parameters (i.e., the SOL_AWC and the CN_2) are estimated in the last iterations according to the suggestion in section 3.3. Moreover, a naive constrained method [*Wang et al*., 2009] is imposed on the states and parameters to avoid violating relevant physical laws or constraints. The smoothing factor (in equation (3)) is $\alpha = 0.99$. Like the synthetic case in section 3, the ensemble spread is inflated by $h = 1.0$ if the standard variance of the ensemble is smaller than 0.05 times the predefined width (Table 2).

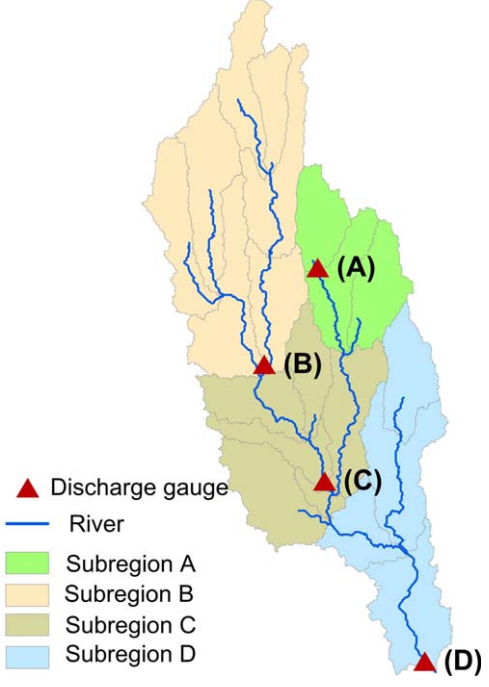

Figure 10. Four subregions divided based on subbasins for localization.

[53] In order to compare the performance of the PU_EnKF and the SU_EnKF on an equal footing, their ensemble sizes are set to 80 and 560, respectively. Note that there are seven loops for the assimilation integration with the PU_EnKF. The performance of data assimilation is evaluated using the time series of the estimation error of streamflow, which is the difference between the ensemble means and the observations (the means minus the observations).

4.4. Results of Data Assimilation

[54] Figure 11 plots the estimation errors of streamflow for the four measurement sites. It is immediately apparent that the PU_EnKF algorithm provides much better estimates of streamflow than the SU_EnKF algorithm, as indicated by the magnitude of error time series, the RMSEs, and the MAEs. Moreover, the PU_EnKF algorithm shows little biased tendency in the estimation as the positive and negative errors appear alternately; whereas, the SU_EnKF algorithm underestimates the streamflow, especially for the peak flood flow. This underestimation may be primarily attributed to the biased parameter estimation.

[55] Figure 12 shows spatial distributions of the final estimates of the parameter CN_2 (CN_2 is the dominant parameter in SWAT, as stated previously). They are mapped with respect to the spatial distribution of land use and soil, since HRUs in SWAT do not hold specific spatial sites. The estimates from the PU_EnKF and the SU_EnKF obviously differ from the initial estimates. The former provides relatively modest, or possibly optimal, estimates. However, the SU_EnKF scheme produces larger estimates, which will lead to significantly biased estimation of peak flow. We have also performed and examined open-loop ensemble simulations that are conditioned on the perturbed parameters and precipitation, but without using observations to calibrate the simulations. Similar to the SU_EnKF, the open-loop integrations also exhibit large errors for peak flow estimation (the results not shown).

[56] To examine the updating process of parameters, we randomly chose an HRU and drew a group of parameter ensembles. Figure 13 exhibits a typical estimation process of CN_2 that is chosen from the 90th HRU in subbasin 18. The ensemble estimates display broad spreads at the beginning, which then diminish as assimilation proceeds, but maintain stable levels after several hundred assimilation steps. In the updating process, the distribution of the ensemble members almost maintains Gaussian properties, as indicated by histograms. This favorable distribution partly benefits from the kernel smoothing method for parameter evolutions. Moreover, the diminishing phenomenon of the spread is further indicated by a global ensemble spread that is the square root of the mean variances of all the parameters in a type [*Chen and Zhang*, 2006]. As shown in Figure 14, the global

Table 2. Model Parameters to be Estimated in Data Assimilation

Parameter (Type)	Description	Scale	Process	Min	Max
CN_2	SCS runoff curve number for moisture condition II	HRU	Runoff	35.0	98.0
CH_K	Effective hydraulic conductivity of channels alluvium (mm/h)	Subbasin	Channel water	0.02	76.0
SOL_AWC	Available water capacity of the soil layer (mm/mm soil)	HRU	Soil	0.0	1.0
surlag	Surface runoff lag coefficient (h)	HRU	Runoff	1.0	10.0
GWQMN	Threshold depth of water in the shallow aquifer required for return flow to occur (mm)	HRU	Groundwater	20.0	1000.0
ESCO	Plant evaporation compensationx factor	HRU	Evaporation	0.0	1.0
ALPHA_BF	Base flow alpha factor (day)	HRU	Lateral water	0.0	1.0

ensemble spreads become more or less stable approximately after 600 steps for the SU_EnKF and 80 steps for the PU_EnKF, which means that the data assimilations have achieved stable estimations for parameters, and there will be no significant improvement in subsequent assimilation steps. This suggests a potential application of using short-period observations to estimate hydrologic parameters as indicated by *Xie and Zhang* [2010], particularly using the PU_EnKF scheme.

4.5. Validation of the Parameter Estimates

[57] Although the two assimilation schemes achieve very different estimates of parameters, it is difficult to explain these estimates within the associated physical context, since SWAT is a conceptual distributed model. To evaluate these estimates of parameters, we design a separate validation in which model predictions are compared against the observation data.

[58] By setting the model parameters with the final estimates, we conduct a single-run streamflow prediction rather than an ensemble prediction, in order to represent a conventional case of model prediction. The prediction is performed for the period from 1 January 2006 to 31 October 2006, because of the data availability from the four streamflow gauges. Moreover, uncertainties posed by both the precipitation and the model structure are not considered. We compare results from three different parameter sets, i.e., the estimates from the PU_EnKF and the SU_EnKF, and the initial guess that is used to produce parameter realizations before data assimilation.

Table 3. Dynamic Hydrologic States and Outputs to be Updated in Data Assimilation

Variable	Description	Scale[a]
Qsufstor	Amount of surface runoff stored or lagged	HRU
Qlatstor	Amount of lateral flow stored or lagged	HRU
Qshall	Amount of shallow water stored or lagged	HRU
Qrchrg	Amount of recharge entering the aquifer	HRU
Qpregw	Amount of groundwater flow into the main channel	HRU
Wsol	Amount of water stored in the soil layer for each HRU	HRU × Nlay[b]
Wr	Amount of water stored in the reach	Subbasin
Wb	Amount of water stored in the bank	Subbasin
SW	Amount of water stored in soil profile	Subbasin
Qr	Amount of water flow out of reach (Streamflow)	Subbasin (Reach)

[a]The hydrologic variables are with respect to the scales to reflect the related hydrologic processes.

[b]Here Nlay is the number of soil layers (Nlay = 4 for this study), and HRU × Nlay means that the soil profile of each HRU is partitioned into Nlay layers.

[59] Figure 15 only shows the results from the period of 1 April 2006 to 31 October 2006, since, in the first 3 months, the basin is in a dry state, and the three simulations do not produce appreciable distinctions. The parameter set from the PU_EnKF produces relatively small errors for peak flow predictions, as well as for base flow, while the parameter set from the SU_EnKF imposes much larger streamflow errors. Moreover, the results provided by the simulation with the initially guessed parameters apparently depart from the observed trajectories. The RMSEs exhibited in Figure 15 also illustrate the improvements achieved by the two assimilation schemes. At the gauge at the basin outlet (Gauge D), for example, the RMSEs have been reduced from 6.731 for the initial-guess scenario, to 4.888 for the SU_EnKF and to 2.393 for the PU_EnKF. These improvements are attributable to proper parameter estimates, which further demonstrate the capability of the PU_EnKF for state-parameter estimation.

5. Summary and Conclusions

[60] The EnKF with state augmentation is susceptible to performance degradation and leads to unsuccessful state-parameter estimation, particularly when the augmented state vector of distributed hydrologic models is of a high dimension. This degradation is primarily caused by spurious correlations for the nonlinear response of hydrologic processes. To capture relatively accurate correlations between states and parameters, we proposed a partitioned update scheme (i.e., the PU_EnKF) according to parameter types with a repeated forecast and assimilation procedure. This scheme was demonstrated with a synthetic case and a real-world case using a distributed hydrologic model (SWAT).

[61] The results from the synthetic experiments clearly showed that the PU_EnKF performs well in state and parameter estimation; in particular, the parameter estimates are close to their truths after finite assimilation steps. The PU_EnKF exhibits its effectiveness that primarily benefits from its partitioned forecast-update scheme rather than the multiassimilation scheme. The combination of the PU_EnKF algorithm and the kernel smoothing scheme for parameter evolution is a preferable strategy for state-parameter estimation. Moreover, the performance of the PU_EnKF is robust to the parameter estimation ordering. In contrast, the SU_EnKF provides unstable parameter estimations due to biased correlation representation, even if all parameters are updated repeatedly at each time step by

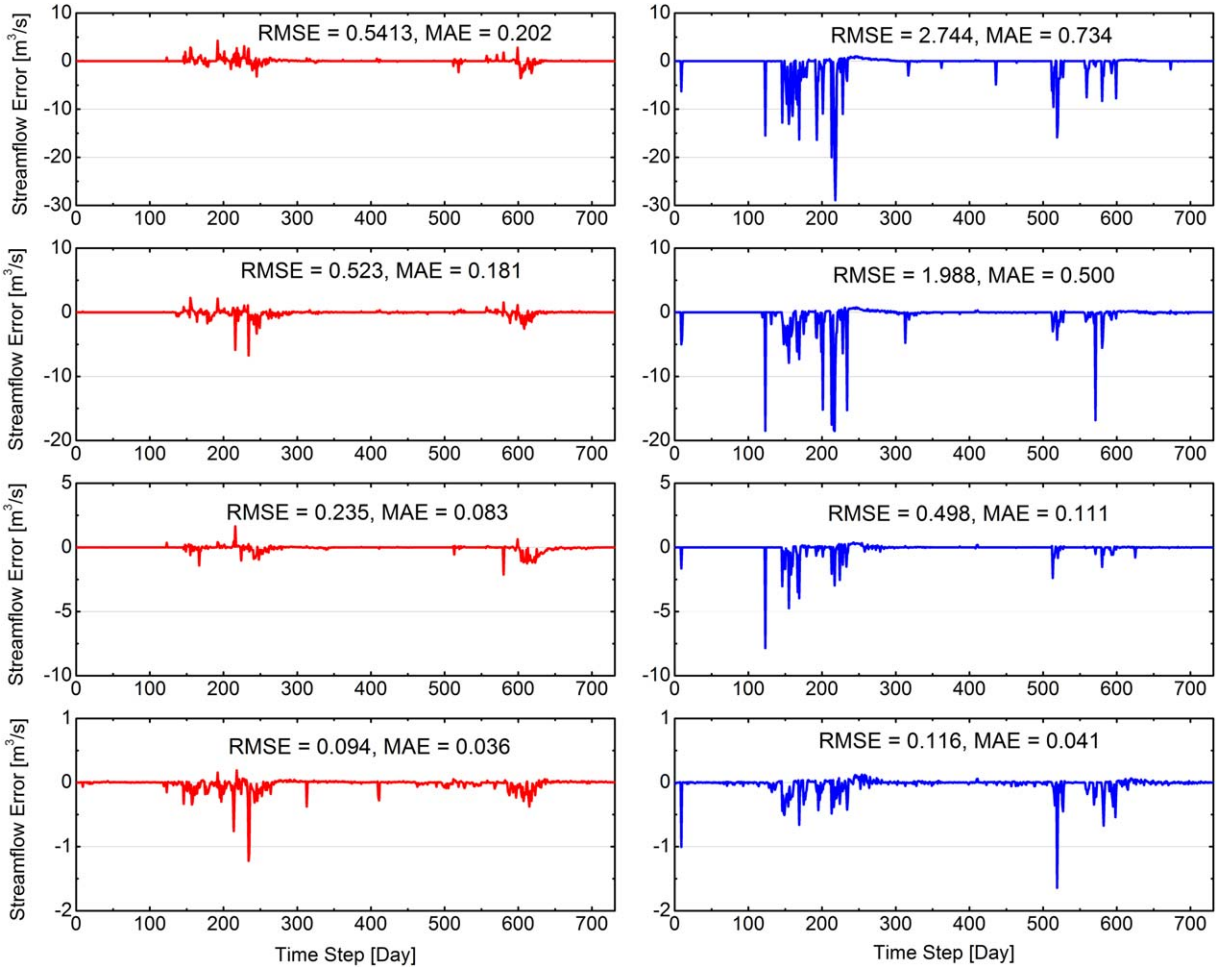

Figure 11. Estimation error of streamflow for the four observation stations (D, C, B, and A, from top to bottom): (left) the PU_EnKF and (right) the SU_EnKF.

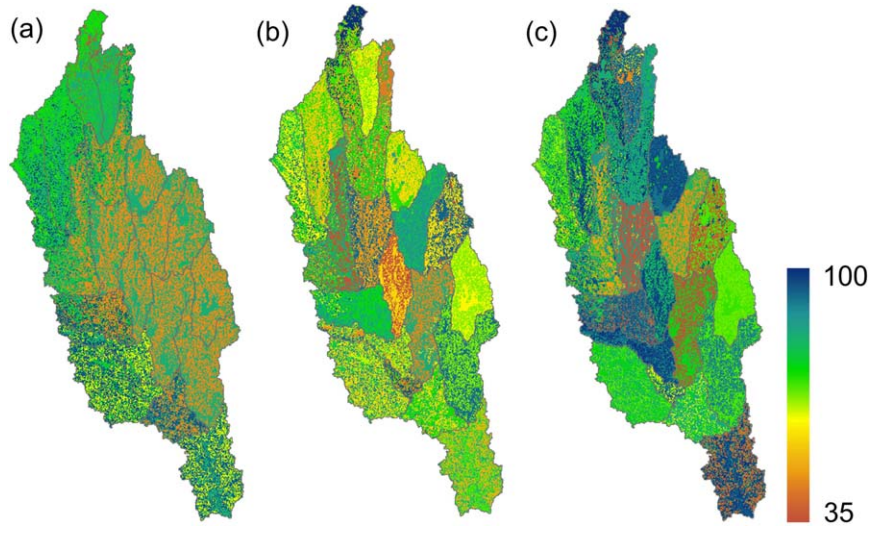

Figure 12. Estimation of parameter CN_2 values for all HRUs, mapped to land use and soil distribution: (a) initial realization for data assimilation; (b) estimation by PU_EnKF; and (c) estimation by SU_EnKF.

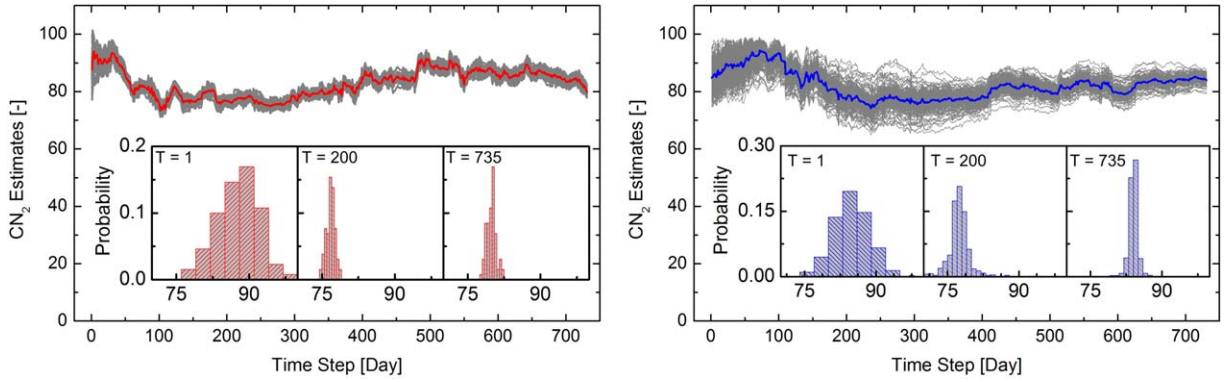

Figure 13. Typical trajectories of CN_2 estimation using the (left) PU_EnKF and the (right) SU_EnKF, and the histograms at the first, 200th, and final steps. The dark gray lines are ensemble members, and the red and blue thick lines are ensemble means.

assimilating the same observations. Although the initial parameter bias is constrained after spin-up assimilation, the SU_EnKF is unable to overcome the instability of parameter estimation.

[62] In the real-world case, the PU_EnKF provides smaller errors for streamflow estimation than does the SU_EnKF, particularly for the peak flow estimation. These errors mainly result from biased parameter estimation. Typically, as the most important type of parameters in SWAT, the parameter values of CN_2 have been overestimated by the SU_EnKF compared to the reasonable estimates of the PU_EnKF. Moreover, stable estimates of parameters can be achieved after a few assimilation steps because of the steady ensemble spread. This also suggests the potential of using short-term observations to obtain appropriate estimates of parameters.

[63] Even though PU_EnKF likely performers better than SU_EnKF for nonlinear problems, they may have similar performance for linear problems. The effectiveness of SU_EnKF has also been illustrated in the literature using hydrologic models of low-dimensional state-parameter vectors, such as lumped hydrologic models [*Dechant and Moradkhani*, 2011; *Leisenring and Moradkhani*, 2011; *Wang et al*., 2009] and land surface models [e.g., *Nie et al*., 2011]. In the synthetic experiments with the simple model in this study, the SU_EnKF also provides acceptable estimation for parameters and states in some measures when comparing the estimation errors with the given model and observation errors. Thus, the SU_EnKF can be optional for low-dimensional problems; however, it may suffer from overconfidence and divergence for state and parameter estimation [*DeChant and Moradkhani*, 2012]. Note that the particle filtering is also useful for state-parameter estimation and has been demonstrated in a few lumped hydrologic models [*Moradkhani et al*., 2005a, 2005b; *Moradkhani and Sorooshian*, 2008]. As a non-Gaussian technique, its performance highly depends on the dimension of the models and the observation errors, and it is restricted by its computational cost [*Han and Li*, 2008]. For distributed hydrologic models, *Xie and Zhang* [2010] documented the success of the SU_EnKF, but only one (type) parameter with respect to surface runoff was considered in the estimation, i.e., CN_2 in SWAT. Considering various parameters in distributed hydrologic models, the PU_EnKF employs an iterative update scheme to reduce the degree of freedom, thereby correctly representing the relationship between states and parameters. Therefore, the PU_EnKF is a beneficial alternative data assimilation scheme for high-dimensional problems.

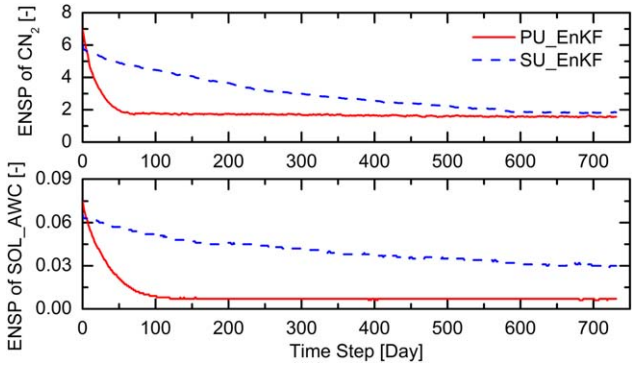

Figure 14. Evolutions of the global ensemble spread (ENSP) of parameters (CN_2 and SOL_AWC). Representative results are shown, while the others exhibit similar processes.

[64] Despite its success, the PU_EnKF, like any other EnKF-based algorithm, is prone to suboptimal solutions of parameters in the real-world cases because it uses a limited number of random realizations to approximate the model and observation errors. It is difficult to thoroughly overcome the problem of parameter equifinality, which means that different parameter values may fit the data equally well [*Beven*, 2006; *Beven and Freer*, 2001b]. For a real-time ensemble prediction, one remedy to this problem is the ensemble simulation/prediction [*Duan et al*., 2007] that is contained in the framework of EnKF. Moreover, this scheme is still restricted by the model and observation error estimation. This can be alleviated by calibrating the error information or by adaptive filtering algorithms [*Crow and Reichle*, 2008; *Reichle et al*., 2008]. In addition, the effectiveness of this scheme may vary with different problems; for long-term data assimilation, it may be computationally expensive due to its repetitious assimilation. In this case, a sensitivity analysis is recommended beforehand to select the most influential parameters to be estimated. The

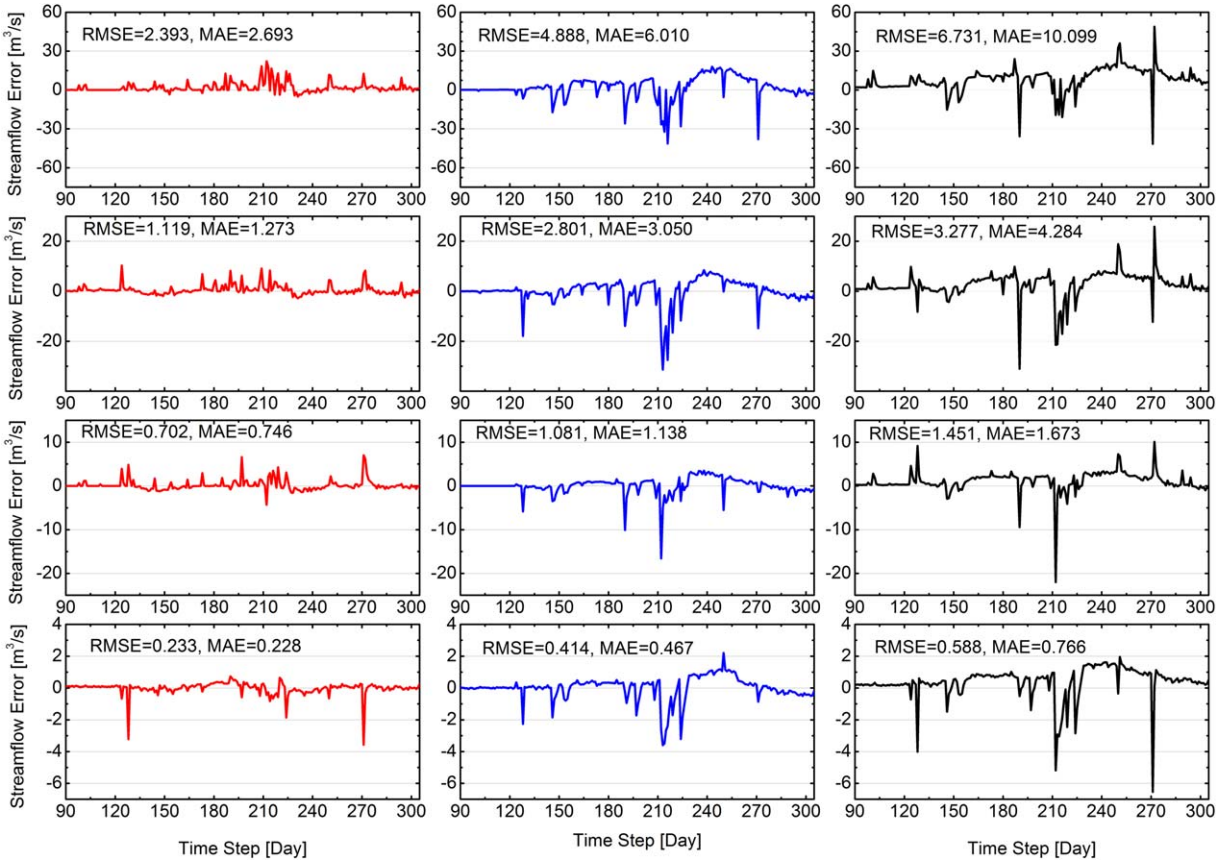

Figure 15. Predicted streamflow errors for the four stations (D, C, B, and A, from top to bottom) from three model runs which uses different parameter sets, i.e., the estimates from (left) the PU_EnKF, (middle) the SU_EnKF, and (right) the initial guess.

PU_EnKF scheme could be a general tool for other distributed hydrologic models, and not just for the SWAT model discussed in this paper. However, this requires further investigation, using other hydrologic models for real-world hydrologic problems.

[65] **Acknowledgments.** We would like to thank the anonymous reviewers for their constructive comments. Qingyun Duan and Hamid Moradkhani also provided helpful suggestions for this study. This work was supported by grants from the National Natural Science Foundation of China (51009001 and 50911130509), the Fundamental Research Funds for the Central Universities (105562GK), and the National High Technology Research and Development Program of China (2013AA121200).

References

Ajami, N. K., Q. Duan, and S. Sorooshian (2007), An integrated hydrologic Bayesian multimodel combination framework: Confronting input, parameter, and model structural uncertainty in hydrologic prediction, *Water Resour. Res.*, *43*, W01403, doi:10.1029/2005WR004745.

Annan, J., J. Hargreaves, N. Edwards, and R. Marsh (2005), Parameter estimation in an intermediate complexity Earth system model using an ensemble Kalman filter, *Ocean Modell.*, *8*(1–2), 135–154.

Arnold, J., P. Allen, and G. Bernhardt (1993), A comprehensive surface-groundwater flow model, *J. Hydrol.*, *142*(1–4), 47–69.

Beven, K. (2006), A manifesto for the equifinality thesis, *J. Hydrol.*, *320* (1–2), 18–36.

Beven, K., and A. Binley (1992), The future of distributed models: Model calibration and uncertainty prediction, *Hydrol. Processess*, *6*(3), 279–298.

Beven, K., and J. Freer (2001a), Equifinality, data assimilation, and uncertainty estimation in mechanistic modelling of complex environmental systems using the GLUE methodology, *J. Hydrol.*, *249*(1–4), 11–29.

Beven, K., and J. Freer (2001b), Equifinality, data assimilation, and uncertainty estimation in mechanistic modelling of complex environmental systems using the GLUE methodology, *J. Hydrol.*, *249*(1–4), 11–29.

Cai, X. L. (2007), Strategy analysis on integrated irrigation water management with RS/GIS and hydrological model, PhD thesis, Wuhan Univ., Wuhan, China.

Chen, M., S. Liu, L. Tieszen, and D. Hollinger (2008), An improved state-parameter analysis of ecosystem models using data assimilation, *Ecol. Modell.*, *219*(3–4), 317–326.

Chen, Y., and D. Zhang (2006), Data assimilation for transient flow in geologic formations via ensemble Kalman filter, *Adv. Water Resour.*, *29*(8), 1107–1122.

Clark, M. P., D. E. Rupp, R. A. Woods, X. Zheng, R. P. Ibbitt, A. G. Slater, J. Schmidt, and M. J. Uddstrom (2008), Hydrological data assimilation with the ensemble Kalman filter: Use of streamflow observations to update states in a distributed hydrological model, *Adv. Water Resour.*, *31*(10), 1309–1324.

Crow, W. T., and R. H. Reichle (2008), Comparison of adaptive filtering techniques for land surface data assimilation, *Water Resour. Res.*, *44*, W08423, doi:10.1029/2008WR006883.

Crow, W. T., and E. Van Loon (2006), Impact of incorrect model error assumptions on the sequential assimilation of remotely sensed surface soil moisture, *J. Hydrometeorol.*, *7*(3), 421–432.

Dechant, C., and H. Moradkhani (2011), Radiance data assimilation for operational snow and streamflow forecasting, *Adv. Water Resour.*, *34*(3), 351–364.

DeChant, C. M., and H. Moradkhani (2012), Examining the effectiveness and robustness of sequential data assimilation methods for quantification of uncertainty in hydrologic forecasting, *Water Resour. Res.*, *48*, W04518, doi:10.1029/2011WR011011.

Duan, Q., S. Sorooshian, and V. Gupta (1992), Effective and efficient global optimization for conceptual rainfall-runoff models, *Water Resour. Res.*, *28*(4), 1015–1031.

Duan, Q., V. Gupta, and S. Sorooshian (1993), Shuffled complex evolution approach for effective and efficient global minimization, *J. Optim. Theory Appl.*, *76*(3), 501–521.

Duan, Q. Y., N. K. Ajami, X. G. Gao, and S. Sorooshian (2007), Multi-model ensemble hydrologic prediction using Bayesian model averaging, *Adv. Water Resour.*, *30*(5), 1371–1386.

Evensen, G. (1994), Sequential data assimilation with a nonlinear quasi-geostrophic model using Monte Carlo methods to forecast error statistics, *J. Geophys. Res.*, *99*(C5), 10,143–10,162.

Evensen, G. (2003), The ensemble Kalman filter: Theoretical formulation and practical implementation, *Ocean Dyn.*, *53*(4), 343–367.

Evensen, G. (2009), *Data Assimilation: The Ensemble Kalman Filter*, Springer, Berlin.

Gassman, P., M. Reyes, C. Green, and J. Arnold (2007), The soil and water assessment tool: Historical development, applications, and future research directions, *Trans. ASABE*, *50*(4), 1211–1250.

Han, X., and X. Li (2008), An evaluation of the nonlinear/non-Gaussian filters for the sequential data assimilation, *Remote Sens. Environ.*, *112*(4), 1434–1449, doi:10.1016/j.rse.2007.07.008.

Helton, J., and F. Davis (2003), Latin hypercube sampling and the propagation of uncertainty in analyses of complex systems, *Reliab. Eng. Syst. Safety*, *81*(1), 23–69.

Holvoet, K., A. van Griensven, P. Seuntjens, and P. A. Vanrolleghem (2005), Sensitivity analysis for hydrology and pesticide supply towards the river in SWAT, *Phys. Chem. Earth, Parts A/B/C*, *30*(8–10), 518–526.

Kalman, R. E. (1960), A new approach to linear filtering and prediction problems, *J. Basic Eng.*, *82*(1), 35–45.

Kavetski, D., S. W. Franks, and G. Kuczera (2004), Confronting input uncertainty in environmental modelling, in *Calibration of Watershed Models, Water Sci. Appl. Ser.*, vol. *6*, edited by Q. Duan et al., pp. 49–68, AGU, Washington, D. C.

Leisenring, M., and H. Moradkhani (2011), Snow water equivalent prediction using Bayesian data assimilation methods, *Stochastic Environ. Res. Risk Assess.*, *25*(2), 253–270.

Liu, F. (2000), Bayesian time series: Analysis methods using simulation-based computation, PhD thesis, Inst. of Stat. and Decis. Sci., Duke Univ., Durham, North Carolina.

Liu, G., Y. Chen, and D. Zhang (2008), Investigation of flow and transport processes at the MADE site using ensemble Kalman filter, *Adv. Water Resour.*, *31*(7), 975–986.

Liu, Y., and H. V. Gupta (2007), Uncertainty in hydrologic modeling: Toward an integrated data assimilation framework, *Water Resour. Res.*, *43*, W07401, doi:10.1029/2006WR005756.

Moradkhani, H., and S. Sorooshian (2008), General review of rainfall-runoff modeling: Model calibration, data assimilation, and uncertainty analysis, in *Hydrological Modelling and the Water Cycle*, edited by S. Sorooshian, K.-L. Hsu, E. Coppola, B. Tomassetti, M. Verdecchia and G. Visconti, pp. 1–24, Springer, Berlin.

Moradkhani, H., K.-L. Hsu, H. Gupta, and S. Sorooshian (2005a), Uncertainty assessment of hydrologic model states and parameters: Sequential data assimilation using the particle filter, *Water Resour. Res.*, *41*, W05012, doi:10.1029/2004WR003604.

Moradkhani, H., S. Sorooshian, H. V. Gupta, and P. R. Houser (2005b), Dual state-parameter estimation of hydrological models using ensemble Kalman filter, *Adv. Water Resour.*, *28*(2), 135–147.

Muleta, M. K., and J. W. Nicklow (2005), Sensitivity and uncertainty analysis coupled with automatic calibration for a distributed watershed model, *J. Hydrol.*, *306*(1–4), 127–145.

Neitsch, S., J. Arnold, J. Kiniry, J. Williams, and K. King (2001), *Soil and Water Assessment Tool Theoretical Documentation Version 2000*, Grassland, Soil and Water Res. Lab., Temple, Tex.

Nie, S., J. Zhu, and Y. Luo (2011), Simultaneous estimation of land surface scheme states and parameters using the ensemble Kalman filter: Identical twin experiments, *Hydrol. Earth Syst. Sci.*, *15*(8), 2437–2457.

Pebesma, E. J., and G. B. M. Heuvelink (1999), Latin hypercube sampling of Gaussian random fields, *Technometrics*, *41*(4), 303–312.

Ponce, V., R. Hawkins, B. Golding, R. Smith, and G. Willeke (1996), Runoff curve number: Hyas it reached maturity?, *J. Hydrol. Eng.*, *1*(1), 11–19.

Rallison, R., and N. Miller (1981), Past, present and future SCS runoff procedure, in *Rainfall Runoff Relationship*, edited by V. P. Singh, pp. 353–364, Water Resour. Publ, Littleton, Colo.

Reed, S., V. Koren, M. Smith, Z. Zhang, F. Moreda, D. J. Seo, and D. Participants (2004), Overall distributed model intercomparison project results, *J. Hydrol.*, *298*(1–4), 27–60.

Refsgaard, J. C., B. Storm, and T. Clausen (2010), Systeme Hydrologique Europeen (SHE): Review and perspectives after 30 years development in distributed physically-based hydrological modelling, *Hydrol. Res.*, *41*(5), 355–377.

Reichle, R., D. McLaughlin, and D. Entekhabi (2002), Hydrologic data assimilation with the ensemble Kalman filter, *Mon. Weather Rev.*, *130*(1), 103–114.

Reichle, R. H., and R. D. Koster (2003), Assessing the impact of horizontal error correlations in background fields on soil moisture estimation, *J. Hydrometeorol.*, *4*(6), 1229–1242.

Reichle, R. H., W. T. Crow, and C. L. Keppenne (2008), An adaptive ensemble Kalman filter for soil moisture data assimilation, *Water Resour. Res.*, *44*, W03423, doi:10.1029/2007WR006357.

Smith, M. B., D. J. Seo, V. I. Koren, S. M. Reed, Z. Zhang, Q. Duan, F. Moreda, and S. Cong (2004), The distributed model intercomparison project (DMIP): Motivation and experiment design, *J. Hydrol.*, *298*(1–4), 4–26.

Troch, P. A., C. Paniconi, and D. McLaughlin (2003), Catchment-scale hydrological modeling and data assimilation, *Adv. Water Resour.*, *26*(2), 131–135.

van Griensven, A., T. Meixner, S. Grunwald, T. Bishop, M. Diluzio, and R. Srinivasan (2006), A global sensitivity analysis tool for the parameters of multi-variable catchment models, *J. Hydrol.*, *324*(1–4), 10–23.

Vrugt, J. A., H. V. Gupta, W. Bouten, and S. Sorooshian (2003), A Shuffled Complex Evolution Metropolis algorithm for optimization and uncertainty assessment of hydrologic model parameters, *Water Resour. Res.*, *39*(8), 1201, doi:10.1029/2002WR001642.

Vrugt, J. A., C. G. H. Diks, H. V. Gupta, W. Bouten, and J. M. Verstraten (2005), Improved treatment of uncertainty in hydrologic modeling: Combining the strengths of global optimization and data assimilation, *Water Resour. Res.*, *41*, W01017, doi:10.1029/2004WR003059.

Wang, D., Y. Chen, and X. Cai (2009), State and parameter estimation of hydrologic models using the constrained ensemble Kalman filter, *Water Resour. Res.*, *45*, W11416, doi:10.1029/2008WR007401.

Weerts, A. H., and G. Y. H. El Serafy (2006), Particle filtering and ensemble Kalman filtering for state updating with hydrological conceptual rainfall-runoff models, *Water Resour. Res.*, *42*, W09403, doi:10.1029/2005WR004093.

West, M. (1993), Mixture models, Monte Carlo, Bayesian updating, and dynamic models, *Comput. Sci. Stat.*, *24*, 325–333.

Xie, X., and Y. Cui (2011), Development and test of SWAT for modeling hydrological processes in irrigation districts with paddy rice, *J. Hydrol.*, *396*(1–2), 61–71.

Xie, X., and D. Zhang (2010), Data assimilation for distributed hydrological catchment modeling via ensemble Kalman filter, *Adv. Water Resour.*, *33*(6), 678–690.

Young, P. C. (2002), Advances in real-time flood forecasting, *Philos. Trans. R. Soc. London A*, *360*(1796), 1433–1450.

Zhang, D. (2002), *Stochastic Methods for Flow in Porous Media: Coping with Uncertainties*, Academic, San Diego, Calif.